Glucose Controls Glucagon Secretion by Regulating Fatty Acid Oxidation in Pancreatic α-Cells

Sarah L. Armour,[1] Alexander Frueh,[1] Margarita V. Chibalina,[2] Haiqiang Dou,[3] Lidia Argemi-Muntadas,[4] Alexander Hamilton,[1,5] Georgios Katzilieris-Petras,[1] Peter Carmeliet,[6,7,8] Benjamin Davies,[9] Thomas Moritz,[4] Lena Eliasson,[5] Patrik Rorsman,[2,3] and Jakob G. Knudsen[1]

Diabetes 2023;72:1446–1459 | https://doi.org/10.2337/db23-0056

Whole-body glucose homeostasis is coordinated through secretion of glucagon and insulin from pancreatic islets. When glucose is low, glucagon is released from α-cells to stimulate hepatic glucose production. However, the mechanisms that regulate glucagon secretion from pancreatic α-cells remain unclear. Here we show that in α-cells, the interaction between fatty acid oxidation and glucose metabolism controls glucagon secretion. The glucose-dependent inhibition of glucagon secretion relies on pyruvate dehydrogenase and carnitine palmitoyl transferase 1a activity and lowering of mitochondrial fatty acid oxidation by increases in glucose. This results in reduced intracellular ATP and leads to membrane repolarization and inhibition of glucagon secretion. These findings provide a new framework for the metabolic regulation of the α-cell, where regulation of fatty acid oxidation by glucose accounts for the stimulation and inhibition of glucagon secretion.

ARTICLE HIGHLIGHTS

- It has become clear that dysregulation of glucagon secretion and α-cell function plays an important role in the development of diabetes, but we do not know how glucagon secretion is regulated.
- Here we asked whether glucose inhibits fatty acid oxidation in α-cells to regulate glucagon secretion.
- We found that fatty acid oxidation is required for the inhibitory effects of glucose on glucagon secretion through reductions in ATP.
- These findings provide a new framework for the regulation of glucagon secretion by glucose.

Circulating glucose levels are under strict control by the release of glucagon and insulin from pancreatic islets. Glucagon secretion is increased when glucose levels are low to stimulate glucose production from the liver. Circulating glucagon levels are also elevated in individuals with obesity and people with diabetes, and this is thought to contribute to the development of hyperglycemia (1–4). Treating hyperglucagonemia with glucagon receptor antagonists lowers HbA_{1c} in patients with diabetes (5), but increases the risk of hepatic steatosis (6) and possibly α-cell hyperplasia (7). However, our limited knowledge of α-cell function has made therapeutic intervention difficult.

Glucose is considered the major intrinsic regulator of glucagon secretion at low glucose (<5 mmol/L). However, the mechanism remains widely debated (8–10). The current hypotheses include, but are not limited to, regulation

[1]Section for Cell Biology and Physiology, Department of Biology, University of Copenhagen, Copenhagen, Denmark
[2]Oxford Centre for Diabetes, Endocrinology and Metabolism, University of Oxford, Churchill Hospital, Oxford, U.K.
[3]Department of Physiology, Sahlgrenska Academy, University of Gothenburg, Gothenburg, Sweden
[4]Novo Nordisk Foundation Center for Basic Metabolic Research, Faculty of Health and Medical Sciences, University of Copenhagen, Copenhagen, Denmark
[5]Department of Clinical Sciences in Malmö, Islet Cell Exocytosis, Lund University Diabetes Centre, Lund University, Malmö, Sweden
[6]Laboratory of Angiogenesis and Vascular Metabolism, Centre for Cancer Biology, Vlaams Instituut voor Biotechnologie (VIB), Department of Oncology, Leuven Cancer Institute, Katholieke Universiteit Leuven, Leuven, Belgium
[7]Laboratory of Angiogenesis and Vascular Heterogeneity, Department of Biomedicine, Aarhus University, Aarhus, Denmark
[8]State Key Laboratory of Ophthalmology, Zhongshan Ophthalmic Center, Sun Yat-Sen University, Guangdong, People's Republic of China
[9]Wellcome Centre for Human Genetics, University of Oxford, Oxford, U.K.

Corresponding author: Jakob G. Knudsen, jgknudsen@bio.ku.dk

Received 19 January 2023 and accepted 16 July 2023

This article contains supplementary material online at https://doi.org/10.2337/figshare.23737635.

© 2023 by the American Diabetes Association. Readers may use this article as long as the work is properly cited, the use is educational and not for profit, and the work is not altered. More information is available at https://www.diabetesjournals.org/journals/pages/license.

of ATP-sensitive K^+ (K_{ATP}) channels (11), store-operated Ca^{2+} channels (12), and reductions in cAMP (13). Common for all is the assumption that at low glucose concentrations, K_{ATP} channels are mostly closed and that inhibition of glucagon release by glucose relies on an increase in ATP derived from glucose oxidation. This creates a paradox, where ATP needs to be high at both low and high glucose concentrations. While previous findings suggest that glucose increases intracellular ATP in α-cells, more recent findings suggest that α-cells rely on fatty acid (FA) oxidation (FAO) for ATP production at low glucose (14) to maintain glucagon secretion. Although glucose and nonesterified FAs (NEFAs) circulate in concentrations of 5–8 mmol/L and 0.07–0.56 mmol/L, respectively (15–17), the mechanisms that control glucose-regulated glucagon secretion are often investigated with glucose as the only substrate (11,13,14,18–27). Here we hypothesize that the effect of glucose on glucagon secretion and α-cell metabolism depends on the presence of NEFA.

RESEARCH DESIGN AND METHODS

Human Islets

All work with human material was approved by the National Committee for the Ethical Approval of Research, Denmark, and the ethics committee at Lund University. Human islets were obtained from the ADI Islet Core Laboratory at the University of Alberta (Edmonton, Alberta, Canada), or Nordic Network for islet transplantation via Human Tissue Laboratory, EXODIAB/LUDC, Lund University (Lund, Sweden). None of the donors had diabetes (Table 1). Islets were cultured at 37°C, 5% CO_2 in RPMI 1640 (61870-010; 10% FBS, 1% penicillin/streptomycin).

Animals

All experiments were approved by the Danish Animal Inspectorate. Mice were housed on a 12–12-h light-dark cycle at 22°C with ad libitum access to standard chow and were 12–20 weeks old. Mice with overexpression of pyruvate dehydrogenase kinase 4 (*Pdk4*) were generated as previously described (28). Briefly, mouse Pdk4 cDNA and rabbit β-globin polyadenylation sequence, preceded by a loxP flanked neomycin cassette, was inserted via PhiC31 recombinase-mediated cassette exchange downstream of the chicken β-actin promoter position at the Gt(ROSA26)Sor locus, in mouse C57BL/6N JM8F6 embryonic stem cells. Recombinant embryonic stem cells were then injected into blastocysts, and the resulting chimeras were bred with C57BL/6J mice to generate the line of conditional Pdk4 overexpression mice.

Table 1—Human donor information

Donor No.	Sex	Age (years)	HbA_{1c} (%)	BMI (kg/m^2)
Donor 1	Female	59	4.8	26.4
Donor 2	Male	32	5.9	26.6
Donor 3	Male	48	5.5	27.5

In these mice, Pdk4 transcription can be activated in a Cre recombinase-dependent manner. The mice carrying the Pdk4 transgene were crossed with mice carrying iCRE under the prepro-glucagon (PPG) promoter (29). Mice with conditional knockout of *Cpt1a* were generated as previously described (30). α-Cell–specific GCamp3 mice were generated as previously described (20). C57Bl6/J mice, referred to as wild-type (WT) mice, were purchased from Janvier Labs (Le Genest-Saint-Isle, France). For in vivo and ex vivo studies using the *Pdk4α* knock-in (KI) and *αCpt1a* mice, results from both sexes were pooled, unless otherwise stated.

Islet Isolation

Mice were euthanized by cervical dislocation, and islets were isolated by Liberase injection (Roche, 05401020001) into the common bile duct, as previously described (14,31), hand-picked into 11 mmol/L glucose RPMI 1640 (61870-010; 10% FBS, 1% penicillin/streptomycin), and incubated at 37°C in 5% CO_2.

Immunohistochemistry

Pancreata from control and Pdk4αKI mice were fixed in 10% neutral buffered formalin (Sigma-Aldrich, HT501128), cryoembedded, and cut into 5-µm sections. Sections were costained for glucagon (1:500; Sigma-Aldrich, G2654) and Pdk4 (dilution 1:50; Protein Tech, 12949-1-Ab) overnight at 4°C. Isolated islets were stained for glucagon, insulin (1:100; Cell Signaling, L6B10) and green fluorescent protein (GFP) for Perceval detection (1:100; Abcam, ab13970). FACS-sorted α-cells were seeded overnight before staining with glucagon (Abcam, ab108426). Secondary antibodies were added before counterstaining with DAPI. Imaging was performed on a Leica SP5-X. Intensity of Pdk4 staining was analyzed in ImageJ software (https://imagej.net/software/fiji/). Sections were blinded and assigned to the respective genotype following analysis to prevent bias.

Viral Constructs

To facilitate reporter expression in α-cells, adenoviruses carrying H2B-GFP or Perceval High Range (HR) under glucagon promoter were created. A GUTR2 construct (32) was used as a template to amplify GCG-H2B-mCherry cassette. The amplified 3.5-kb fragment was cloned into pGEM, sequenced, and subsequently subcloned into shuttle pDUAL2-V5His-bGH (Vector Biolabs, Malvern, PA). *Eco*RI restriction site was then introduced downstream of the reporter. PercevalHR was amplified from FUGW-PercevalHR obtained from Addgene (no. 49083) and cloned into pGEM. H2B-mCherry was cut from the GCG promoter cassette in pDUAL2-V5His-bGH using *Not*I and *Eco*RI and substituted with PercevalHR or H2B-GFP. Sequences of all constructs were verified. Adenoviruses were produced by Vector Biolabs.

Confocal Microscopy

Time-lapse imaging was performed on whole islets using a Leica SP5-X with a 40× objective. For viral induction

and dye loading, islets were incubated and parameters set as stated in Table 2. Viral infection with PercevalHR (33) or GFP was used to specifically identify changes in α-cells. Islets were (unless otherwise stated) preincubated for 30 min in 1 mmol/L glucose Krebs Ringer Buffer (KRB; 140 mmol/L NaCl, 4.6 mmol/L KCl, 2.6 mmol/L $CaCl_2$, 1.2 mmol/L $MgCl_2$, 1 mmol/L NaH_2PO_4, 25 mmol/L $NaHCO_3$, 10 mmol/L HEPES, pH7.4, and 6.6 mg/mL FA-free BSA) (6). Islets were perifused with KRB containing a physiological relevant mix and concentration of FAs (0.36 mmol/L NEFA) (21% palmitate, 45.5% oleic acid, and 22.8% linoleic acid bound to FA-free BSA in a 3.6:1 molar ratio) (16), FA-free BSA only, or no BSA at 0.2 mL/min at 35°C. All solutions contained D-glucose and/or carbonyl cyanide-4- (trifluoromethoxy)phenylhydrazone as indicated. Images were taken every 5 min for ATP-Red and every 2 min for all other experiments. Fiji/ImageJ was used for analysis where fluorescence was normalized to the initial condition (F/F_0), and the last 6 min of each condition was averaged for statistical analysis. Calcium imaging was performed as previously described (20), and islets were perfused with KRB, with or without 0.36 mmol/L NEFA and D-glucose, as indicated, at a rate of 0.2 mL/min at 35°C. Images were acquired in 1.28-Hz intervals. GCaMP calcium traces of individual islet cells were analyzed using MATLAB R2018b. Peaks were identified by using built-in MATLAB functions msbackadj(), trapz(), and findpeaks(), a minimal peak height of two times the average intensity of all cell traces, a minimum peak distance of two and width of one, with a peak prominence of at least 1 SD of the individual cell trace.

FACS

Islets were isolated from B6J mice and cultured overnight in the incubator (800 islets in 2.5 mL, 7 mmol/L glucose RPMI 1640 [61870-010], 10% FBS, and 1% penicillin/streptomycin). The next day, islets were dispersed using 50% TrypLE for 5 min in a 37°C water bath. Then, 7 mmol/L glucose RPMI was added before centrifugation and dispersion in KRB + 3 mmol/L glucose + 5% serum. Dispersed cells were subjected to single-cell sorting based on their size and autofluorescence. The sort was gated for exclusion of duplets and other cell aggregates based on side scatter (SSC) and forward scatter (FSC). α-Cells were distinguished from non–α-cells based on size (FSC parameter) (34) and autofluorescence (FITC parameter) (35) and sorted into 7 mmol/L glucose RPMI.

[U-^{13}C]Glucose Metabolomics

Cells were centrifuged and resuspended in 7 mmol/L glucose RPMI, and 10,000 cells were incubated at 37°C in 5% CO_2 in 100 μL medium to recover for 1 h. The medium was then replaced with KRB containing 1 mmol/L glucose and 0.36 mmol/L NEFA for 30 min before being replaced with KRB containing 1 mmol/L or 5 mmol/L [U-^{13}C]glucose and 0.36 mmol/L NEFA for 2 h. Cells were gently centrifuged, and the supernatant was removed. Then, 300 μL 90% high-performance liquid chromatography-grade methanol was added, and cell pellets were frozen at −80°C. After three cycles of snap-freezing in liquid nitrogen and vortexing, cells were incubated on ice to precipitate proteins. Samples were then centrifuged at 12,000 rpm at 4°C for 15 min, and the supernatant was transferred to liquid chromatography–mass spectrometry and evaporated to completeness under a stream of N_2. Ketovaline (not detected in samples in a pilot experiment) was added as an internal standard together with sample extract. Dried extracts were derivatizatized with 3-nitrophenylhydrazine essentially according to Hodek et al. (36) and thereafter analyzed by using an ultrahigh performance liquid chromatography system (Agilent 1290 Infinity II) connected to a Bruker timsTOF Pro mass spectrometer (Bruker, Bremen, Germany) operated in negative ionization mode. Extraction and derivatization blanks and calibration curves were derivatized and analyzed as samples. Data processing was performed with Bruker Compass DataAnalysis 5.2 software and TASQ 2021b (Bruker). Calculation of [^{13}C] labeling, including correction for natural isotopes, was done according to Lindén et al. (37).

Electrophysiology

Electrical activity of α-cells within intact mouse islets was measured using a perforated-patch technique. During the experiments, the islets were perfused with an extracellular solution containing (mmol/L) 140 NaCl, 3.6 KCl, 1.3 $CaCl_2$, 0.5 $MgSO_4$, 10 HEPES, 0.5 NaH_2PO_4, and 5 $NaHCO_3$ at pH 7.4, with NaOH and glucose/NEFA as indicated. The temperature of the solution was controlled between 32 and 34°C. The solution within the pipette contained (in mmol/L) 76 K_2SO_4, 10 KCl, 10 NaCl, 1 $MgCl_2$, and 5 HEPES (pH 7.35

Table 2—Time-lapse imaging parameters

Virus/dye	Cat no., vendor	Loading conditions	Excitation wavelength (nm)	Emission wavelength (nm)
PercevalHR	N/A	24–48 h 37°C, 5% CO_2	488	510–600
GFP	N/A	24–48 h 37°C, 5% CO_2	488	510–601
ATP-Red	SCT045, Sigma-Aldrich	10 μmol/L, 2.5 μL/mL pluronic, 30 min 37°C	510	540–600
SNARF-5F	S23923, Thermo Fisher	10 μmol/L, 2.5 μL/mL pluronic, 30 min 37°C	514	570–670
pHRodoRed	P35372, Thermo Fisher	50 μL 30 min RT	560	500–600

N/A, not applicable; RT, room temperature.

using KOH). The pore-forming antibiotic amphotericin B (240 μg/mL) was included in the intracellular buffer to achieve membrane perforation. α-Cells were distinguished by their functional fingerprinting (38). Electrophysiological measurements were performed using an EPC-10 patch-clamp amplifier (HEKA Electronics, Ludwigshafen/Rhein, Germany) and PatchMaster 2 × 91 software.

Hormone Secretion

Glucagon secretion was measured from groups of 10 islets/replicate. Following isolation, islets were incubated for 1 h in 11 mmol/L glucose RPMI, washed once with KRB containing 0 mmol/L glucose, and preincubated in 2 mmol/L glucose KRB with 0.36 mmol/L NEFA, unless otherwise indicated, for 1 h at 37°C in 5% CO_2. Islets were then incubated sequentially at 1 mmol/L and 5 mmol/L glucose with 0.36 mmol/L NEFA, or as indicated, for 1 h. The supernatant was collected, and islets were harvested in acid ethanol and sonicated. Glucagon and insulin were determined using U-PLEX insulin and glucagon kits (Meso Scale Diagnostics; K15145C-3 or K15303K-4), according to the manufacturer's instructions.

FAO

FAO was measured from 50 islets from WT or αCPT1a knock-out mice (αCPT1aKO) and preincubated in 1 mmol/L glucose with 0.36 mmol/L NEFA, using radiolabeled palmitic acid [9,10-^{3}H(N)] (Perkin Elmer), as previously described (14).

In Vivo Measurements

Body weight, blood glucose, and blood ketones were measured between 8 A.M. and 10 A.M. using a Contour NEXT glucose meter (Bayer) and FreeStyle Precision ketone meter (Abbott).

Glucose Tolerance Test

Glucose tolerance tests were performed after a 6-h fast (6 A.M.–12 P.M.). Mice were injected with D-glucose (2 g/kg; Sigma-Aldrich) in sterile PBS, and blood glucose was measured at 0, 30, 60, 90, and 120 min using a Contour NEXT (Bayer). Blood was collected at 0 and 30 min on ice into aprotinin (Sigma-Aldrich, A11S3), centrifuged at 2600*g* at 4°C for 10 min, and plasma was collected and stored at −80°C. Plasma glucagon levels were measured using the R-PLEX glucagon assay (Meso Scale Diagnostics, F201K-3, L45SA-2-2).

Statistical Analysis

All data are presented as mean ± SEM. All statistics were performed using GraphPad Prism 9 software (GraphPad Software, San Diego, CA). Values outside of 2 SDs were considered outliers and excluded. Specific statistical tests and post hoc analyses are stated in each figure legend.

Data and Materials Availability

Data and materials from this study will be available upon reasonable request.

RESULTS

NEFA Are Required for Glucagon Secretion

The effect of single FAs on glucagon secretion has previously been investigated (39,40). Here we explored how NEFA, in a physiologically relevant mix and concentration, would affect glucose-regulated glucagon secretion. Islets store FAs as triglycerides (41), which can potentially be used for FAO at low glucose. We therefore preincubated WT islets at 5 mmol/L glucose, 1 mmol/L glucose, or 1 mmol/L glucose supplemented with 0.36 mmol/L NEFA. In islets preincubated in 5 mmol/L glucose, an increase in glucose from 1 to 5 mmol/L reduced glucagon secretion (Fig. 1*A*). When islets from the same mice were preincubated in 1 mmol/L glucose, glucagon secretion was both lower at 1 mmol/L glucose and not reduced in response to 5 mmol/L (Fig. 1*A*). However, adding 0.36 mmol/L NEFA to the 1 mmol/L glucose preincubation restored glucose-induced inhibition of glucagon (Fig. 1*A*), without changes in glucagon content (Fig. 1*B*). These findings were not due to changes in insulin secretion (Supplementary Fig. 1*A* and *B*). The effect of NEFA on glucagon secretion at 1 mmol/L glucose was dose dependent and higher at 0.36 mmol/L than at 0 mmol/L NEFA, following a preincubation with the indicated amount of NEFA at 1 mmol/L glucose (Fig. 1*C*). No differences in secretion were observed at 5 mmol/L glucose, and glucose was only repressive in the presence of 0.36 mmol/L NEFA (Fig. 1*C* and *D*). The presence of NEFA also affected glucose-stimulated insulin secretion in the presence of 0.07 mmol/L NEFA (Supplementary Fig. 1*C* and *D*). Islets also maintained the expected response to 10 mmol/L glucose in the presence of 0.36 mmol/L NEFA, lowering glucagon and stimulating insulin secretion (Supplementary Fig. 1*E–H*). The glucose-induced reduction in glucagon secretion in the presence of NEFA was correlated with reduced FAO measured in isolated mouse islets, preincubated in 1 mmol/L glucose with 0.36 mmol/L NEFA, when glucose was increased from 1 mmol/L to 5 mmol/L (Fig. 1*E*). Collectively, this suggests that α-cells rely on the presence of NEFA to maintain the inhibitory effect of glucose on glucagon secretion.

Glucose Lowers Intracellular ATP in α-Cells

We explored how addition of NEFA affected intracellular ATP by expressing the ATP sensor PercevalHR (33) specifically in α-cells (Fig. 2*A* and *B*). Exposing mouse or human islets to 0.36 mmol/L NEFA in the presence of 1 mmol/L glucose increased intracellular ATP in α-cells (Fig. 2*C–F*). When glucose levels were then increased to 5 mmol/L in the presence of 0.36 mmol/L NEFA, intracellular ATP in α-cells was reduced (Fig. 2*C–F*). The observed reduction in ATP was not an artifact due to changes in intracellular pH (Supplementary Fig. 2*A–D*). Similar data were obtained using ATP-Red 1 dye (42) in α-cells with nuclear GFP expression (Supplementary Fig. 2*F–H*). In these experiments, the non-GFP cells tended to increase fluorescence intensity (Supplementary Fig. 2*G* and *H*), as is expected for non–α-cells (24). The effect of glucose on ATP in α-cells required the presence of NEFA as preincubation

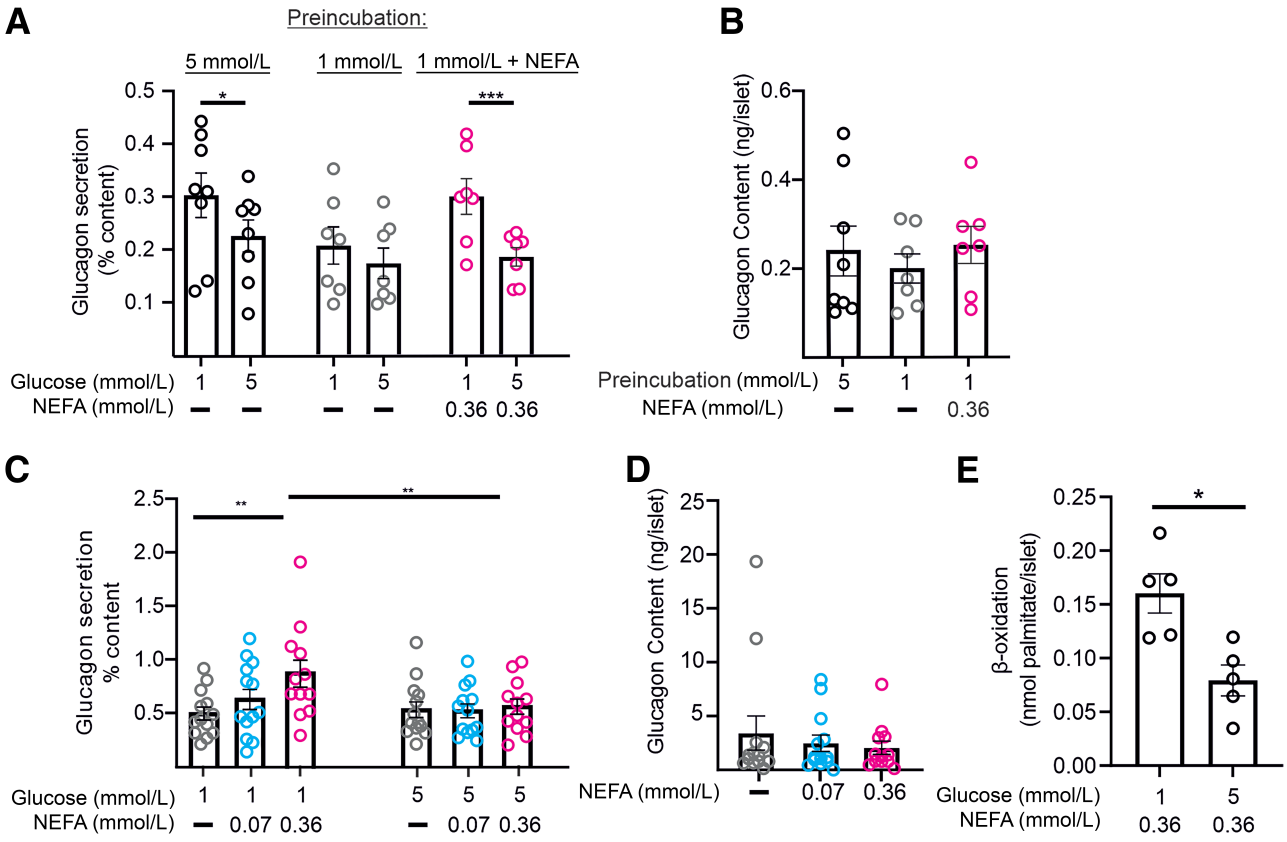

Figure 1—NEFAs are required for glucagon secretion. *A*: Glucagon secretion in response to 1 and 5 mmol/L glucose, with or without 0.36 mmol/L NEFA, from WT islets preincubated at 5 mmol/L or 1 mmol/L glucose, with or without 0.36 mmol/L NEFA (n = 7–8 mice). *B*: Glucagon content for *A*. *C*: Glucagon secretion in response to 1 and 5 mmol/L glucose with 0 mmol/L (gray), 0.07 mmol/L (cyan), or 0.36 mmol/L (magenta) NEFA from WT islets following preincubation in 1 mmol/L glucose with 0 mmol/L (gray), 0.07 mmol/L (cyan), or 0.36 mmol/L (magenta) NEFA (n = 12–13 mice). *D*: Glucagon content for *C*. *E*: β-Oxidation measured in WT islet preincubated in 1 mmol/L glucose with 0.36 mmol/L NEFA and exposed to 1 or 5 mmol/L glucose in the presence of 0.36 mmol/L NEFA (n = 5 mice). All data are represented as mean ± SEM. *P < 0.05, **P < 0.01, ***P < 0.001. (See also Supplemental Fig. 1.) Statistics performed were two-way ANOVA with Šidák post hoc test (*A* and *C*), one-way ANOVA (*B* and *D*), and paired t test (*E*).

of islets at 1 mmol/L glucose removed the reduction in intracellular ATP at both 5 mmol/L glucose and 20 mmol/L glucose (Fig. 2*G*–*J*). The response to glucose was variable in these cells, which could suggest that the degree of intracellular FA depletion may differ between individual α-cells. When WT islets were preincubated in 3 mmol/L glucose, which would spare FA availability, intracellular ATP also decreased in response to 20 mmol/L glucose (Fig. 2*K* and *L*). Notably, these ATP measurements were performed in a buffer containing BSA (6.6 mg/mL), which is required to bind NEFA. Previous ATP measurements that show increased intracellular ATP in response to increased glucose were performed without the addition of BSA (11,14,19,21,43). Indeed, when the ATP measurements were made in the absence of BSA in our experimental system, increasing from 1 to 20 mmol/L glucose increased intracellular ATP (Supplementary Fig. 2*I*). This suggested that α-cell function may be affected by the presence of BSA. To test this, we preincubated islets in 5 mmol/L glucose, with and without BSA, in the absence of 0.36 mmol/L NEFA. In the presence of BSA, glucagon secretion responded as expected (Supplementary Fig. 2*J*). However, complete removal of BSA impaired secretion at both 1 mmol/L and 5 mmol/L glucose (Supplementary Fig. 2*J*). These differences were present without changes in glucagon content (Supplementary Fig. 2*K*) or insulin secretion and content (Supplementary Fig. 2*L*–*M*). Together, these data suggest that under physiological conditions, α-cells use FAs for ATP production and that elevations of extracellular glucose lead to reductions in intracellular ATP.

Glucose Metabolism in α-Cells Supports the Glucose FA Cycle

Normal fuel homeostasis requires reciprocal regulation of glucose and FAO. In the fed state, FAO is inhibited by the increased availability of glucose through the glucose-FA cycle (44–46). The pathway requires pyruvate, derived from glycolysis, to enter the tricarboxylic acid cycle (TCA). Once pyruvate is converted to acetyl-CoA by pyruvate dehydrogenase (PDH), it is condensed with oxaloacetate by citrate synthase to form citrate. Citrate is either used in the TCA cycle or exported to the cytosol, where it acts as substrate for malonyl-CoA synthesis. Production of malonyl-CoA near the mitochondrial membrane leads to inhibition of carnitine palmitoyl 1a (CPT1a)

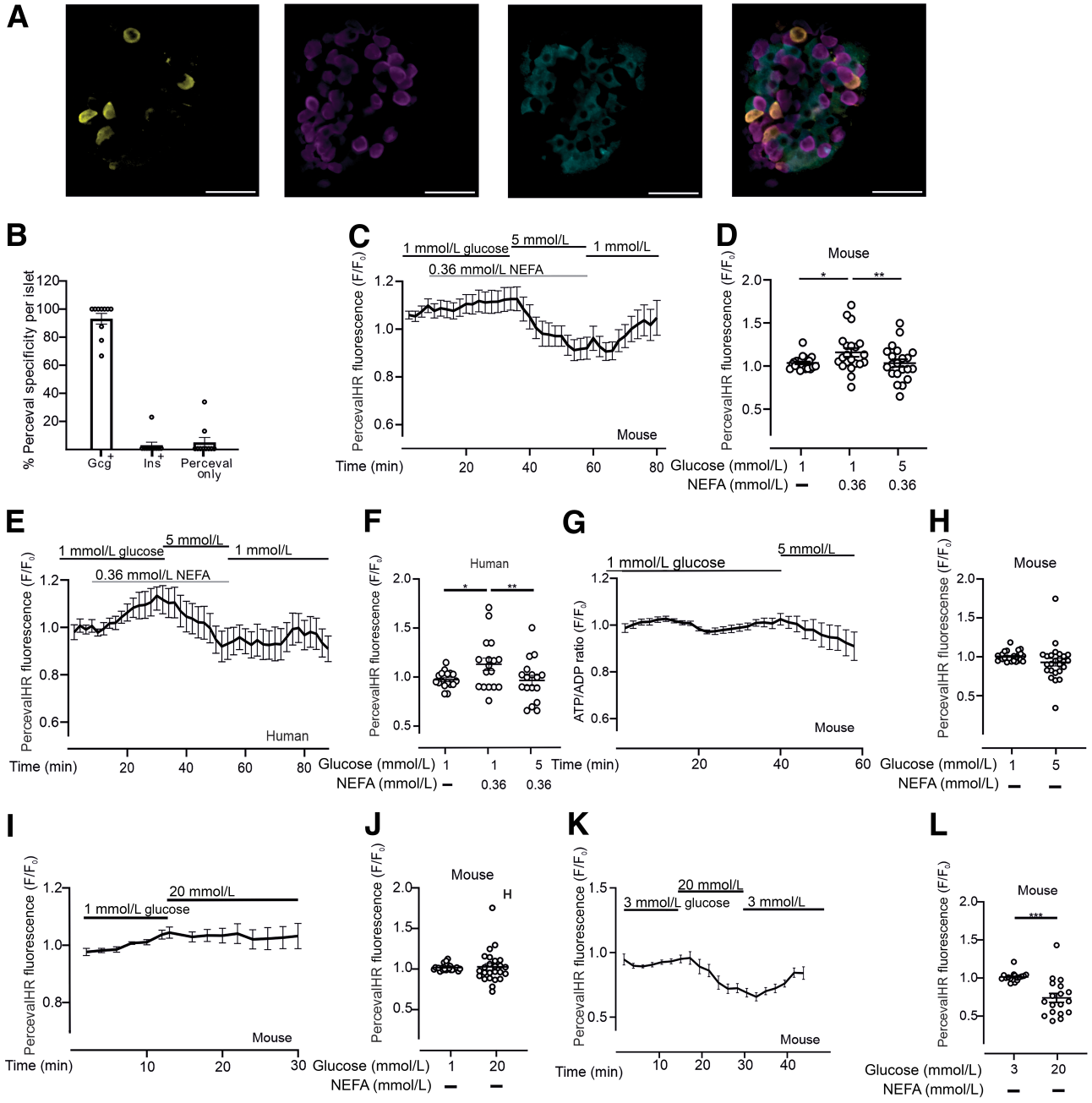

Figure 2—Glucose lowers intracellular ATP in α-cells. *A*: Representative images of isolated islets stained for Perceval (yellow), glucagon (magenta), and insulin (cyan); scale bar = 50 μm. *B*: Quantification of Perceval expression in glucagon and insulin-positive cells (n = 10 islets from three mice). *C*: Average ATP fluorescence measured specifically in α-cells in isolated islets from WT mice in the presence of 0.36 mmol/L NEFA (n = 25 cells from three experiments). *D*: Dot plots of the last three frames in each condition in *C*. *E*: Average ATP fluorescence measured specifically in α-cells in isolated islets from human donors in the presence of 0.36 mmol/L NEFA (n = 17 cells from three experiments). *F*: Dot plots of the last three frames in each condition in *E*. *G*: Average ATP fluorescence measured specifically in α-cells in islets from WT mice in the absence of NEFA and perfused with 1 mmol/L and 5 mmol/L glucose (n = 17 cells from three experiments). *H*: Dot plots of the last three frames in each condition in *G*. *I*: Average ATP fluorescence measured specifically in α-cells in islets from WT mice in the absence of NEFA and perfused with 1 mmol/L and 20 mmol/L glucose (n = 25 cells from three experiments). *J*: Dot plots of the last three frames in each condition in *I*. *K*: Average ATP fluorescence measured specifically in α-cells in islets from WT mice, preincubated in 3 mmol/L glucose, in response to 3 and 20 mmol/L glucose (n = 15 cells from three experiments). *L*: Dot plots of the last three frames in each condition in *K*. All data are represented as mean ± SEM. *P < 0.05, **P < 0.01, ***P < 0.001. (See also Supplemental Fig. 2.) Statistics were performed with one-way ANOVA with the Tukey post hoc test in *D*, *F*, *H*, *J*, and *L*.

and thereby inhibits long-chain FAO (46). Therefore, to understand how glucose lowers intracellular ATP in α-cells, we used stable isotope glucose tracer metabolite profiling. To obtain a pure fraction, α-cells were FACS sorted using flavin-adenine dinucleotide autofluorescence (35). Unlike previously, here sorting was done in 3 mmol/L glucose KRB with 5% FBS. Under these

conditions, flavin-adenine dinucleotide fluorescence is high in other islet cells, and α-cells can be sorted as the least fluorescent fraction (Fig. 3*A*). This led to an α-cell fraction with 89% purity, confirmed by glucagon staining. To understand how glucose is metabolized in α-cells, the sorted α-cell fraction was preincubated in 1 mmol/L glucose with 0.36 mmol/L NEFA and subsequently transferred to 1 or 5 mmol/L [U-^{13}C]glucose with 0.36 mmol/L NEFA for 2 h (Fig. 3*A*).

Analysis by mass spectrometry revealed that the content of all measured metabolites, except for citrate, increased or trended toward an increase in 5 mmol/L compared with 1 mmol/L glucose (Fig. 3*B*). The percentage of ^{13}C enrichment was only increased in α-ketoglutarate (α- KG) and trended toward an increase in citrate (P = 0.101), while the enrichment for succinate decreased (Fig. 3*C*). The similar citrate content and small increase in ^{13}C enrichment could suggest that citrate is being used to generate other metabolites not measured here. The increased percentage of ^{13}C enrichment in α-KG could suggest that citrate may be converted to α-KG. Alternatively, cataplerosis of citrate could explain why there is no increase in the total content of the metabolite (Fig. 3*D*). The combination of increased α-KG and decreased succinate

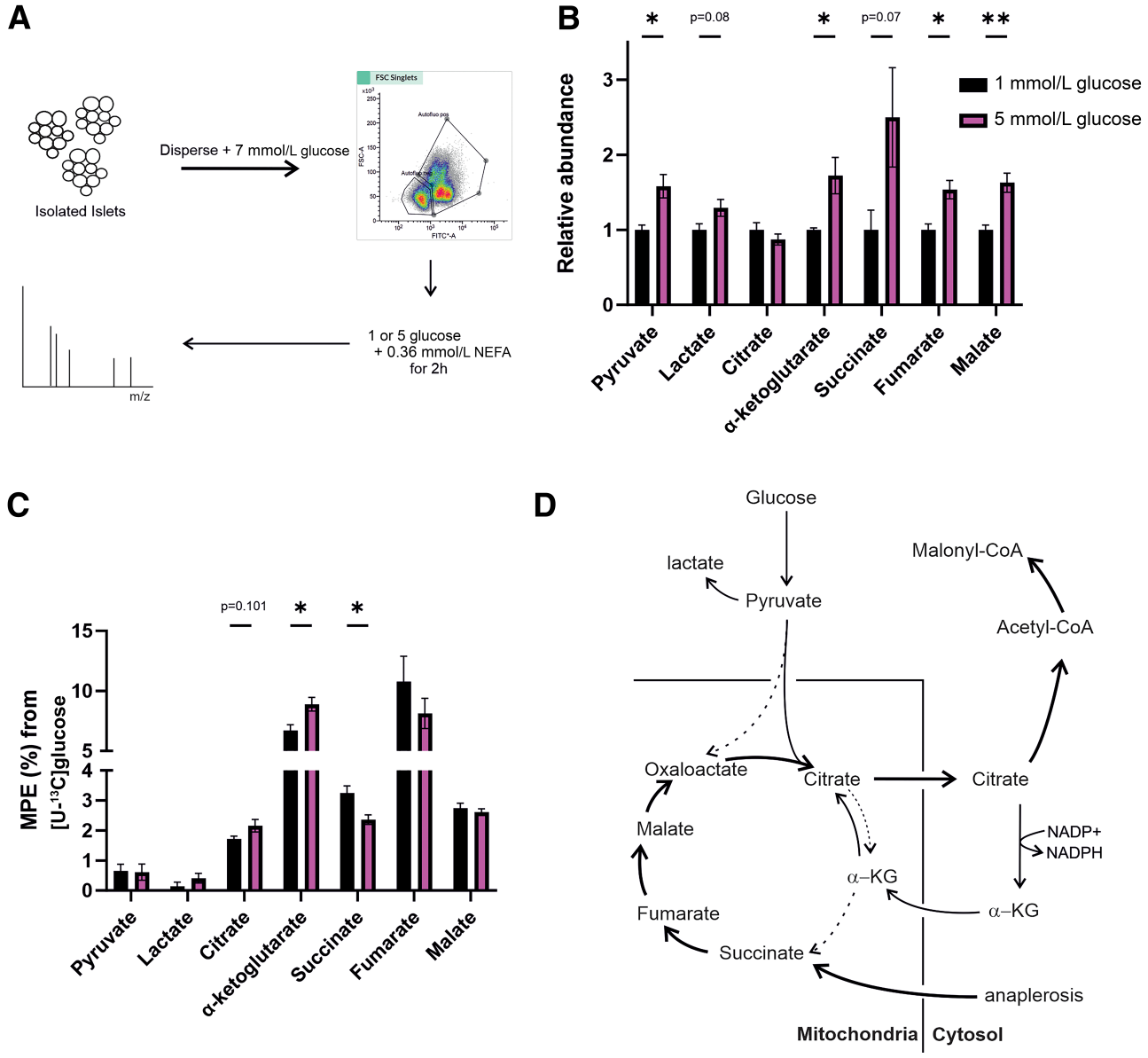

Figure 3—Increased glucose metabolism leads to citrate–α-ketoglutarate cycling in α-cells. *A*: Schematic of experimental approach. *B*: Relative abundance of intracellular metabolites in FACS-sorted α-cells exposed to 1 or 5 mmol/L glucose with 0.36 mmol/L NEFA. *C*: Molar percentage enrichment from [U-^{13}C]glucose in FACS-sorted α-cells exposed to 1 or 5 mmol/L glucose with 0.36 mmol/L NEFA. *D*: Proposed model for glucose metabolism in α-cells. All data presented are mean ± SEM. *$P < 0.05$, **$P < 0.01$. Statistics were performed with the Student *t* test (*B* and *C*).

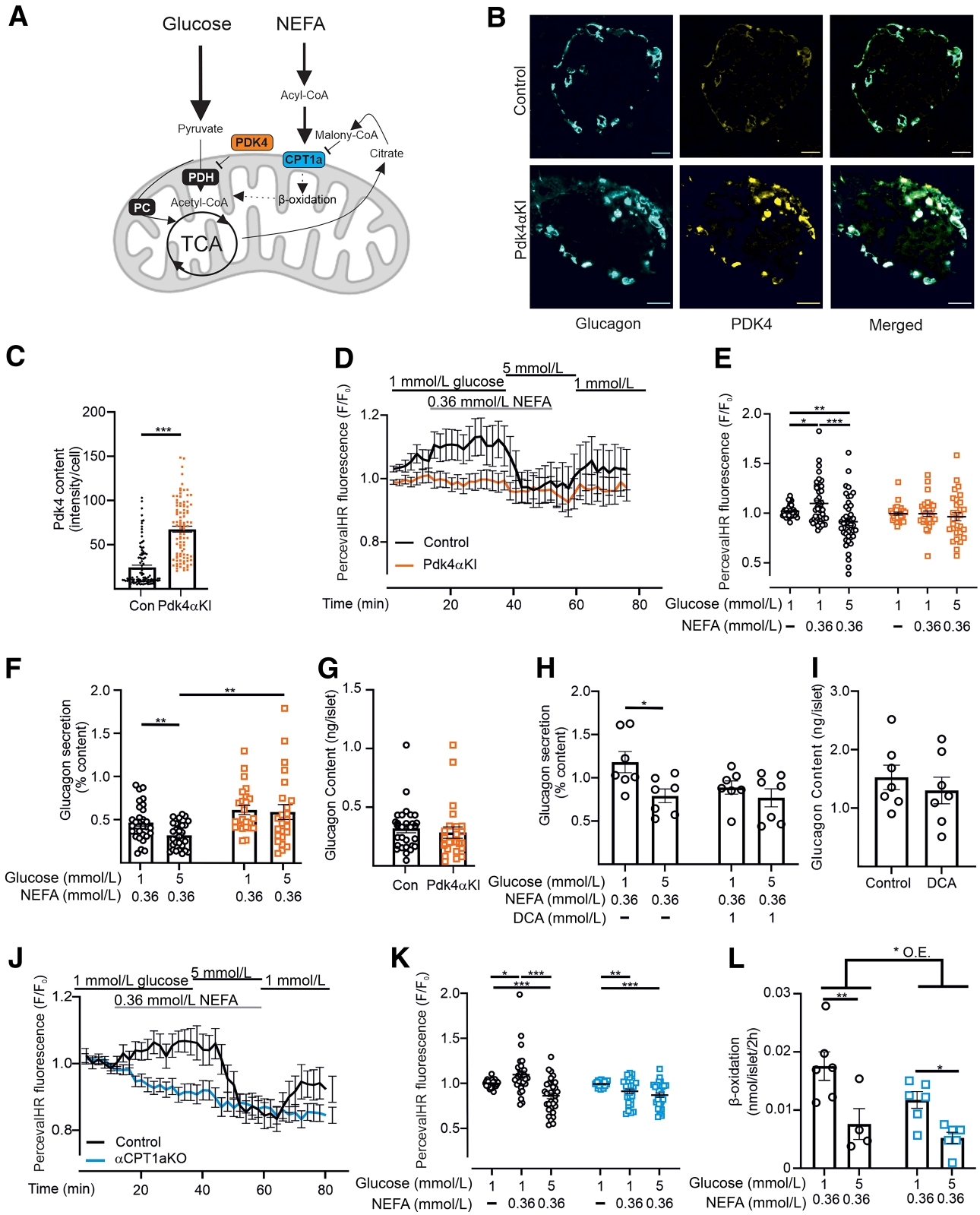

Figure 4—Regulation of FAO is vital for glucose-induced glucagon repression. *A*: A depiction of the interaction between glucose and FAO pathways. PC, pyruvate carboxylase. *B*: From left to right: glucagon (cyan), Pdk4 (yellow), and composite staining in pancreatic sections from control and Pdk4αKI mice. Scale bar = 25 μm. *C*: Pdk4 staining intensity measurements for control (Con) and Pdk4αKI mice (n = 4 mice). *D*: Average ATP fluorescence measured specifically in α-cells in isolated islets from control and Pdk4αKI mice (n = 43 and 30 cells from three to four experiments for control and Pdk4αKI, respectively). *E*: Dot plots of the last three frames of each condition in *D*. *F*: Glucagon secretion from whole islets isolated from control and Pdk4αKI mice in response to 1 or 5 mmol/L glucose in the presence of 0.36 mmol/L NEFA (n = 29 and 25 mice for control and Pdk4αKI, respectively). *G*: Glucagon content for *F*. *H*: Glucagon secretion at 1 and

enrichment suggests that the increases in total concentrations of fumarate, malate, and succinate content may be derived from anaplerotic metabolism. On the basis of the findings in this experimental setup, it is likely that a proportion of citrate is used in the glucose FA cycle or for FA synthesis (Fig. 3*D*).

Glucose Regulates Glucagon Secretion Through PDH and CPT1a

For glucose to contribute to the glucose FA cycle, pyruvate derived from glucose must enter the TCA cycle as oxaloacetate through pyruvate carboxylase or as acetyl-CoA through PDH. The two metabolites can then be condensed by citrate synthase to form citrate. The activity of PDH is determined partly through inhibitory phosphorylation by pyruvate dehydrogenase kinases (PDK) (Fig. 4*A*). Mouse and human α-cells both express high levels of *Pdk4* mRNA compared with other islet cell types (47,48). PDK4 expression is regulated by changes in substrate availability, and consequently, expression is increased in both skeletal muscle (49) and islets (50) during fasting. To determine whether the glucose-FA cycle is important for the effect of glucose on intracellular ATP and glucagon secretion, we generated a mouse model in which *Pdk4* was specifically overexpressed in α-cells (Pdk4αKI). In these mice, the higher PDH phosphorylation would lead to lower influx of pyruvate into the TCA cycle through PDH. PDK4 staining intensity was observed exclusively in α-cells and was twofold higher in Pdk4αKI mice than in controls (Fig. 4*B* and *C*). In these mice, the glucose-induced reduction in intracellular ATP (Fig. 4*D* and *E*) and glucagon secretion (Fig. 4*F*) was lost, without changes in glucagon content (Fig. 4*G*). In addition, the loss of glucose-induced suppression of glucagon secretion in Pdk4αKI mice led to an increase in insulin secretion at 5 mmol/L (Supplementary Fig. 3*A* and *B*), supporting observations that glucagon can potentiate insulin secretion at low glucose concentrations (51). This suggests that PDK4 plays a key role in the regulation of glucagon secretion and that entry of pyruvate as acetyl-CoA into the TCA cycle is important for the reduction of glucagon secretion and intracellular ATP in α-cells. These findings were confirmed by treatment of islets with the PDK inhibitor dichloroacetate, which removed the effect of 5 mmol/L glucose on glucagon secretion (Fig. 4*H*).

*Cpt1a*KO in α-cells leads to decreased long-chain FAO and reduced glucagon secretion at low glucose (14), identical to the effects observed when islets are incubated with low substrate levels (Fig. 1*A*). We therefore investigated the effect of glucose on ATP levels in islets from mice with *Cpt1a*KO specifically in α-cells (αCPT1aKO). Intracellular ATP did not change in α-cells from these mice when exposed to 0.36 mmol/L NEFA or 5 mmol/L glucose, but instead continuously decreased (Fig. 4*J* and *K*), suggesting that α-cells rely on FAO to maintain ATP, as previously observed (14). Some studies have suggested that inhibition of mitochondrial FAO can activate peroxisomal FAO (52–54). We therefore measured whole-islet FAO in control and αCPT1aKO mice at 1 and 5 mmol/L glucose. FAO in whole islets was lower in αCPT1aKO mice at 1 mmol/L glucose and was unaffected by 5 mmol/L glucose (Fig. 4*K*). These findings indicate that the glucose-FA cycle is active in α-cells and that glucose inhibits glucagon secretion by lowering FAO and intracellular ATP.

To test whether *PDK4* expression in α-cells contributes to the regulation of glucagon secretion in vivo, we measured blood glucose and plasma glucagon in Pdk4αKI mice (Fig. 5). Glucose tolerance and plasma glucagon levels were unaffected in male and female Pdk4αKI mice (Fig. 5*A*–*I*). However, unlike controls, glucagon levels failed to reduce in female Pdk4αKI mice after glucose administration (Fig. 5*I*). This was also the case when sexes were combined to increase statistical power (Fig. 5*C*). No changes in body weight, blood glucose, or ketones were observed between genotypes (Fig. 5*J*–*L*). This suggests that, while PDK4 expression in α-cells is an important regulator of glucose-regulated glucagon secretion, it is not enough to drive the development of hyperglycemia or hyperketonemia in vivo.

Glucose Repolarizes α-Cells to Inhibit Glucagon Secretion

Pancreatic α-cells express K_{ATP} channels (48,55). It was previously suggested that closure of the channel leads to reduced action potential height (via voltage gated Na^+ channels), reduced Ca^{2+} influx, and inhibition of glucagon secretion, a mechanism that would require increased ATP in response to glucose. The observation that glucose decreased intracellular ATP in the presence of NEFA therefore prompted us to investigate the electrical activity in α-cells under these experimental conditions. The addition of 0.36 mmol/L NEFA at 1 mmol/L glucose had little effect on plasma membrane potential (Fig. 6*A*–*C*). Unlike in control recordings without NEFA and BSA (Fig. 6*A*), adding 5 mmol/L glucose in the presence of 0.36 mmol/L NEFA repolarized the membrane (Fig. 6*B* and *C*) and reduced the firing frequency of action potentials (Fig. 6*D*). Subsequent addition of the K_{ATP} channel blocker tolbutamide (100 μmol/L) caused a rapid and strong depolarization (Fig. 6*B* and *C*). This could indicate that the reduction in ATP caused by increasing glucose levels leads to

5 mmol/L glucose following treatment with or without dichloroacetate (DCA; $n = 7$ mice). *I*: Glucagon content for *H*. *J*: Average ATP fluorescence measured specifically in α-cells in isolated islets from control and αCPT1aKO mice ($n = 32$ and 30 cells from three to four experiments in control and αCPT1aKO, respectively). *K*: Dot plots of the last three frames of each condition in *J*. *L*: β-Oxidation measured in αCPT1aKO islets exposed to 1 or 5 mmol/L glucose in the presence of 0.36 mmol/L NEFA ($n = 7$–8 mice). All data are represented as mean ± SEM. *$P < 0.05$, **$P < 0.01$, ***$P < 0.001$, *O.E., overall effect of genotype, $P < 0.05$. (See also Supplementary Fig. 3.) Statistics performed were unpaired *t* test (*C*, *G*, and *I*), two-way ANOVA with the Tukey (*E* and *K*) or Šidák (*F* and *H*) post hoc test, and mixed-effects analysis with the Šidák post hoc test (*L*).

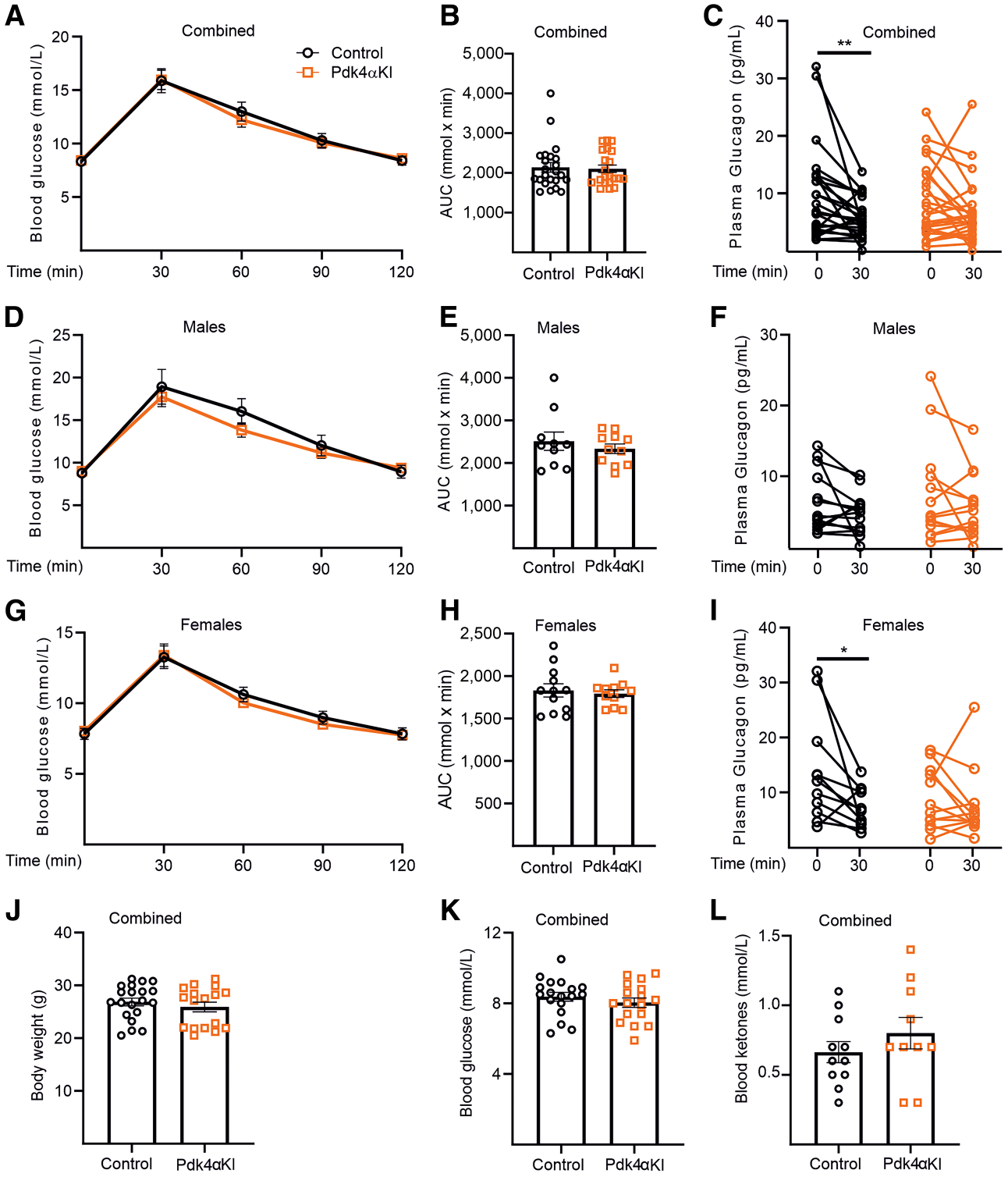

Figure 5—Overexpression of Pdk4 in α-cells affects glucose-regulated glucagon secretion in vivo. *A*: Intraperitoneal (i.p.) glucose tolerance test in control and Pdk4αKI mice (n = 22 for control and Pdk4αKI). *B*: Area under the curve (AUC) for *A*. *C*: Plasma glucagon at 0 and 30 min after i.p. glucose injection (n = 25–26 mice). *D–F*: Data from female mice in *A–C* (n = 12 and 11 for control and Pdk4αKI, respectively in *D* and *E* and n = 11 and 12 for control and Pdk4αKI, respectively in *F*. *G* and *H*: Data from male mice in *A–C* (n = 10 and 11 for control and Pdk4αKI, respectively, in *F* and n = 14 for control and Pdk4αKI in *H*). *J*: Body weight measurements in control and Pdk4αKI mice (n = 17–20 mice). *K*: Blood glucose measurements in control and Pdk4αKI mice (n = 17–18 mice). *L*: Blood ketone measurements in control and Pdk4αKI mice (n = 10–11 mice). All data are represented as mean ± SEM. *$P < 0.05$, **$P < 0.01$. Statistics performed were unpaired t test (*B*, *E*, *H*, *J*, *K*, and *L*) and two-way ANOVA with the Šidák post hoc test (*C*, *F*, and *I*).

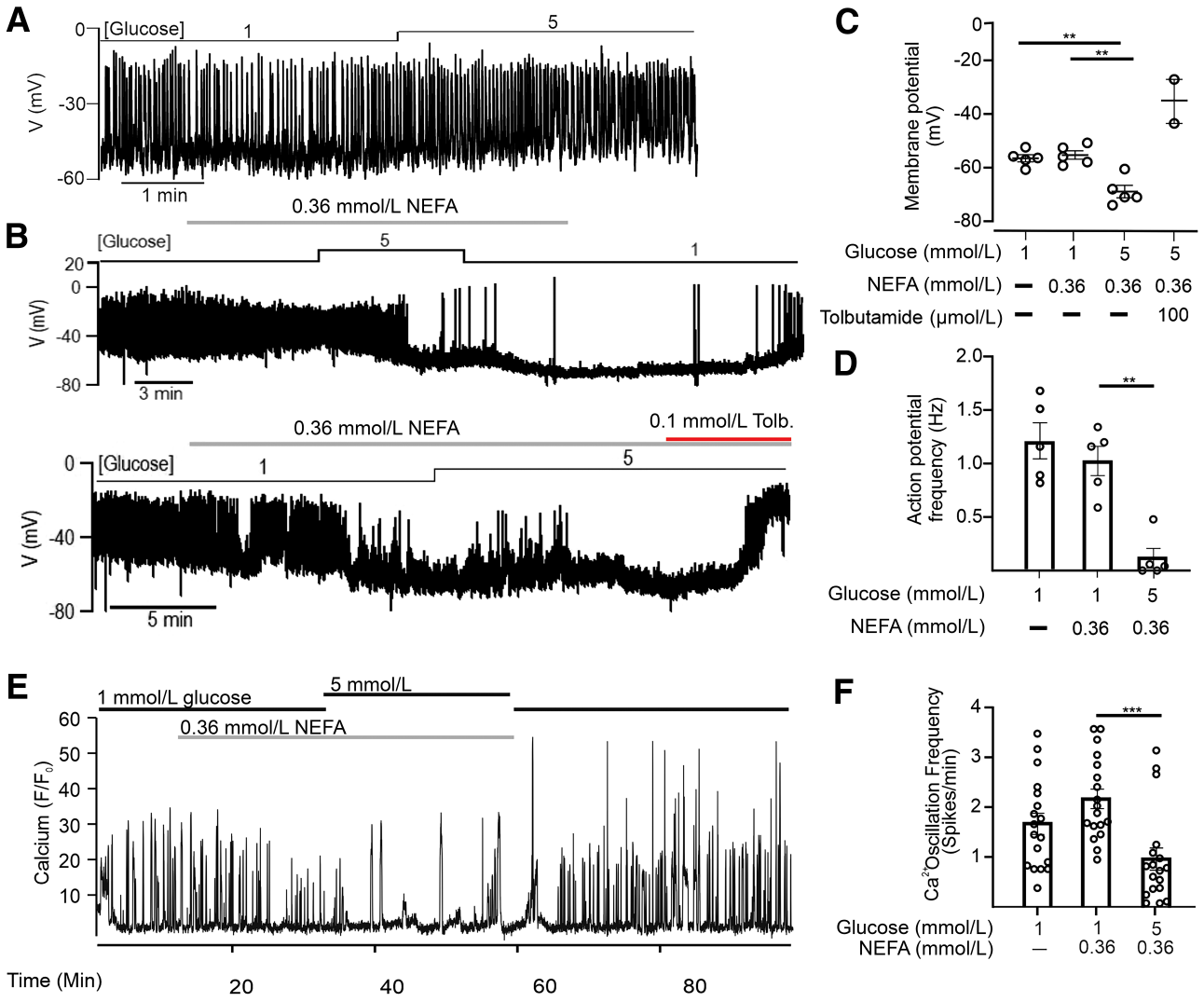

Figure 6—Glucose-induced reduction in ATP repolarizes the plasma membrane in α-cells. *A*: Representative trace of membrane potential measurements in α-cells from intact islets in response to 1 or 5 mmol/L glucose without 0.36 mmol/L NEFA. *B*: Representative traces of membrane potential measurements in α-cells in response to 1 or 5 mmol/L glucose with 0.36 mmol/L NEFA and with or without tolbutamide (Tolb). *C*: Minimum potential measurements from *B* (n = 2–5 cells from three mice). *D*: Action potential frequency measurements from *B* (n = 5 cells from three mice). *E*: Representative trace of calcium oscillations in an α-cells in intact WT islets. *F*: Accumulated data from *E* measuring calcium spike frequency (n = 18 cells from three experiments). All data are represented as mean ± SEM. $^{**}P < 0.01$, $^{***}P < 0.001$. Statistics performed were one-way ANOVA with the Tukey (*C*, *D*, and *F*) post hoc test.

opening of K_{ATP} channels and suggests that membrane potential in α-cells is more negative than previously reported (11). Electrical activity (11) and FAs (40) have both been suggested to regulate glucagon secretion through changes in cytosolic calcium. To investigate whether the addition of 0.36 mmol/L NEFA affected this parameter, we used mice expressing the cytosolic calcium sensor GCaMP3 specifically in α-cells (20). The addition of 0.36 mmol/L NEFA did not affect oscillation frequency in α-cells at 1 mmol/L. Increasing glucose to 5 mmol/L lowered oscillation frequency (Fig. 6*E* and *F*) as expected, in line with previous observations recorded in the absence of NEFA (20). This suggests that at low glucose, the membrane potential is depolarized and that increasing glucose repolarizes the plasma membrane to inhibit electrical activity, calcium entry, and glucagon secretion.

DISCUSSION

Here we propose that the regulation of ATP production in α-cells is highly dependent on enzymes that promote FAO, such as PDK4 and CPT1a. We find that inhibition of pyruvate entry into the TCA cycle as acetyl-CoA, or FA transport into the mitochondria, disconnects changes in glucose levels from changes in ATP production and glucagon secretion. Based on the observations made here, we suggest that glucose regulates glucagon secretion, not by increasing intracellular ATP, but by inhibiting FAO to lower intracellular ATP.

Our findings suggest that in α-cells, FAO is subject to suppression from glucose, as suggested by the glucose-FA cycle. Despite this, α-cells do oxidize glucose to some extent (56,57), at least in the absence of other substrates

and BSA, where increases in extracellular glucose results in ATP production (11,19,21,24,58). However, we show here that in the absence of BSA, α-cells do not secrete much glucagon and do not respond to glucose. While it is not clear why BSA is important for α-cell function, albumin has previously been shown to impact both intracellular lipid, pH, and redox homeostasis (59,60). Depleting endogenously released FAs by adding FA-free BSA to dispersed β-cells has been shown to prevent signaling that stimulates Ca^{2+} oscillations and insulin secretion (33). However, here we observed intact regulation of glucagon secretion with FA-free BSA when whole islets are preincubated in 5 mmol/L glucose, suggesting that this is not occurring in the current experimental paradigm. Whether this discrepancy is due to differences in the experimental paradigm or the two cell types is unclear.

Previous hypotheses of how glucose regulates glucagon secretion suggest that increased ATP from glucose oxidation leads to membrane depolarization in α-cells (11,22). However, as with the previous measurements of ATP, these experiments were performed with glucose as the only substrate. The findings we present here show that glucose repolarizes the plasma membrane in α-cells when applied in the presence of NEFA, consistent with the observed reduction in ATP under the same experimental conditions. The finding that this effect was reversed by tolbutamide suggests it reflects activation of K_{ATP} channels. It has previously been suggested that a reduction in intracellular ATP could lead to reduced Na^+/K^+ pump activity (14); however, this would lead to a depolarization of the membrane, unlike what we see here. It is, therefore, more likely that activation of K_{ATP} channels drives the change in membrane potential in α-cells in response to increased glucose levels. In addition, the current observation that ATP is reduced may also be aligned with the proposed reduction in intracellular cAMP in α-cells (13). While, the apparent K_m of adenylate cyclase for ATP is ∼0.6 mmol/L (61), for some isoforms, the K_m is substantially altered when bound to $G_{\alpha s}$ (62) supporting the possibility that lowering of intracellular ATP could contribute to the lowering cAMP. The lower cAMP could also be caused by increases in intracellular FAs as a consequence of the lower FAO at higher glucose, as adenylate cyclase in other tissues has been suggested to be inhibited by increases in intracellular FA levels (59).

Concentrations of 5 mmol/L glucose and 0.36 mmol/L NEFA mimic plasma levels of macronutrients after an overnight fast; however, after a glucose challenge, postprandial NEFA levels may be as low as 0.07 mmol/L, with plasma glucose concentrations of 8 mmol/L in human subjects (17). Under conditions with 0.07 mmol/L NEFA, we observed lower glucagon secretion at low glucose and no effect of increasing glucose concentrations. This suggests that the lowering of plasma levels of glucagon in response to a glucose tolerance test may also be driven by changes in FA availability. This is supported by the ex vivo experiments presented here. However, overexpression of PDK4 in α-cells results in a rather mild phenotype. That PDK4 overexpression in α-cells alone is not enough to drive the development of hyperglycemia or hyperketonemia in vivo is not surprising. Other models of impaired glucagon secretion also have relatively mild phenotypes (7,14,21,63). In the case of this model, this may reflect that paracrine factors also contribute to the inhibition glucagon secretion. Despite this, our data indicate that changing PDH activity in α-cells can affect circulating glucagon levels. Thus, α-cells may rely on sensing circulating levels of FA as well as glucose. However, it should be considered that other substrates, such as amino acids, could also contribute and thereby regulate glucagon secretion in α-cells (64).

In conclusion, we propose a framework for α-cell metabolism and glucose-regulated glucagon secretion, reciprocal to that observed in β-cells (65), in which the metabolic phenotype of α-cells enables a specialized glucose response, which lowers intracellular ATP and leads to reduced glucagon secretion through activation of K_{ATP} channels and repolarization of the plasma membrane. This model of α-cell metabolism and glucagon secretion suggests that α-cells can act as sensors of changes in both circulating glucose and NEFA concentrations.

Acknowledgments. The authors thank Dorthe Nielsen (University of Copenhagen) for technical assistance during data collection, Professor Leanne Hodson and Dr. Katherine Pinnick (University of Oxford) for scientific advice, and Professor Seung Kim (Stanford University) for providing the GUTR2 construct used for live cell imaging experiments. Imaging experiments were performed at the Centre for Advanced Bioimaging (CAB) at the University of Copenhagen.

Funding. A.H. is supported by a fellowship from Svenska Sällskapet for Medicinsk Forskning (SSMF). Financial support for the transgenic core at the Wellcome Centre for Human Genetics was provided by the Wellcome Trust Core Award Grant Number 203141/Z/16/Z. P.C. is supported by long term structural funding - Methusalem funding by the Flemish government, the Fund for Scientific Research-Flanders (FWO-Vlaanderen), European Research Council Advanced Research Grant EU-(ERC743074), and a Novo Nordisk Foundation (Denmark) NNF Laureate Research Grant. T.M. is supported by the Novo Nordisk Foundation (grant no. NNF18CC0034900) L.E. is supported by the Swedish Research grant (SRA-Exodiab and project grant), the Swedish Foundation for Strategic Research (IRC-LUDC), and The Swedish Diabetes Foundation. P.R. is supported by the Swedish Research Council, the Helmsley Trust, and the Medical Research Council (MRC), J.G.K. is supported by a Novo Nordisk Fonden Excellence Emerging Investigator Grant- Endocrinology & Metabolism (no. 0054300) and an Independent Research Fund Denmark Sapere Aude Fellowship (no. 0169-00067B).

Duality of Interest. No potential conflicts of interest relevant to this article were reported.

Author Contributions. S.L.A., A.F., M.V.C., H.D., L.A.-M., A.H., G.K.-P., T.M., and J.G.K. contributed to the investigation. S.L.A., A.F., M.V.C, H.D., L.A.-M., A.H., G.K.-P., P.C., B.D., T.M., L.E., P.R., and J.G.K. reviewed and edited the manuscript. S.L.A. and J.G.K. conceptualized the study. S.L.A. and J.G.K. conceived the experimental design. S.L.A. and J.G.K. wrote the original draft. M.V.C., P.C., B.D., L.E., and P.R. contributed materials. J.G.K. is the guarantor of this work and, as such, had full access to all the data in the study and takes responsibility for the integrity of the data and the accuracy of the data analysis.

Prior Presentation. Parts of this study were presented as an abstract at the 56th Annual Meeting of the European Association for the Study of Diabetes, virtual meeting, 21–25 September 2020, and at the 81st Scientific Sessions of the American Diabetes Association, virtual meeting, 25–29 June 2021.

References

1. Marliss EB, Aoki TT, Unger RH, Soeldner JS, Cahill GF Jr. Glucagon levels and metabolic effects in fasting man. J Clin Invest 1970;49:2256–2270
2. Starke AAR, Erhardt G, Berger M, Zimmermann H. Elevated pancreatic glucagon in obesity. Diabetes 1984;33:277–280
3. Unger RH, Cherrington AD. Glucagonocentric restructuring of diabetes: a pathophysiologic and therapeutic makeover. J Clin Invest 2012;122:4–12
4. Faerch K, Vaag A, Holst JJ, Glümer C, Pedersen O, Borch-Johnsen K. Impaired fasting glycaemia vs impaired glucose tolerance: similar impairment of pancreatic alpha and beta cell function but differential roles of incretin hormones and insulin action. Diabetologia 2008;51:853–861
5. Kazda CM, Ding Y, Kelly RP, et al. Evaluation of efficacy and safety of the glucagon receptor antagonist LY2409021 in patients with type 2 diabetes: 12- and 24-week phase 2 studies. Diabetes Care 2016;39:1241–1249
6. Guzman CB, Zhang XM, Liu R, et al. Treatment with LY2409021, a glucagon receptor antagonist, increases liver fat in patients with type 2 diabetes. Diabetes Obes Metab 2017;19:1521–1528
7. Gelling RW, Du XQ, Dichmann DS, et al. Lower blood glucose, hyperglucagonemia, and pancreatic α cell hyperplasia in glucagon receptor knockout mice. Proc Natl Acad Sci U S A 2003;100:1438–1443
8. Gylfe E. Glucose control of glucagon secretion-'There's a brand-new gimmick every year'. Ups J Med Sci 2016;121:120–132
9. Gylfe E. Glucose control of glucagon secretion: there is more to it than KATP channels. Diabetes 2013;62:1391–1393
10. Zhang Q, Dou H, Rorsman P. 'Resistance is futile?' - paradoxical inhibitory effects of K_{ATP} channel closure in glucagon-secreting α-cells. J Physiol 2020;598:4765–4780
11. Zhang Q, Ramracheya R, Lahmann C, et al. Role of KATP channels in glucose-regulated glucagon secretion and impaired counterregulation in type 2 diabetes. Cell Metab 2013;18:871–882
12. Liu Y-J, Vieira E, Gylfe E. A store-operated mechanism determines the activity of the electrically excitable glucagon-secreting pancreatic α-cell. Cell Calcium 2004;35:357–365
13. Yu Q, Shuai H, Ahooghalandari P, Gylfe E, Tengholm A. Glucose controls glucagon secretion by directly modulating cAMP in alpha cells. Diabetologia 2019;62:1212–1224
14. Briant LJB, Dodd MS, Chibalina MV, et al. CPT1a-dependent long-chain fatty acid oxidation contributes to maintaining glucagon secretion from pancreatic islets. Cell Rep 2018;23:3300–3311
15. Green CJ, Pramfalk C, Charlton CA, et al. Hepatic de novo lipogenesis is suppressed and fat oxidation is increased by omega-3 fatty acids at the expense of glucose metabolism. BMJ Open Diabetes Res Care 2020;8:e000871
16. Pinnick KE, Collins SC, Londos C, Gauguier D, Clark A, Fielding BA. Pancreatic ectopic fat is characterized by adipocyte infiltration and altered lipid composition. Obesity (Silver Spring) 2008;16:522–530
17. Frayn KN, Coppack SW, Humphreys SM, Clark ML, Evans RD. Periprandial regulation of lipid metabolism in insulin-treated diabetes mellitus. Metabolism 1993;42:504–510
18. Barg S, Galvanovskis J, Göpel SO, Rorsman P, Eliasson L. Tight coupling between electrical activity and exocytosis in mouse glucagon-secreting alpha-cells. Diabetes 2000;49:1500–1510
19. Basco D, Zhang Q, Salehi A, et al. α-Cell glucokinase suppresses glucose-regulated glucagon secretion. Nat Commun 2018;9:546
20. Kellard JA, Rorsman NJG, Hill TG, et al. Reduced somatostatin signalling leads to hypersecretion of glucagon in mice fed a high-fat diet. Mol Metab 2020;40:101021
21. Knudsen JG, Hamilton A, Ramracheya R, et al. Dysregulation of glucagon secretion by hyperglycemia-induced sodium-dependent reduction of ATP production. Cell Metab 2019;29:430–442.e4
22. MacDonald PE, De Marinis YZ, Ramracheya R, et al. A K ATP channel-dependent pathway within α cells regulates glucagon release from both rodent and human islets of Langerhans. PLoS Biol 2007;5:e143
23. Vergari E, Knudsen JG, Ramracheya R, et al. Insulin inhibits glucagon release by SGLT2-induced stimulation of somatostatin secretion. Nat Commun 2019;10:139
24. Li J, Yu Q, Ahooghalandari P, et al. Submembrane ATP and Ca2+ kinetics in α-cells: unexpected signaling for glucagon secretion. FASEB J 2015;29:3379–3388
25. Omar-Hmeadi M, Lund P-E, Gandasi NR, Tengholm A, Barg S. Paracrine control of α-cell glucagon exocytosis is compromised in human type-2 diabetes. Nat Commun 2020;11:1896
26. Le Marchand SJ, Piston DW. Glucose suppression of glucagon secretion: metabolic and calcium responses from α-cells in intact mouse pancreatic islets. J Biol Chem 2010;285:14389–14398
27. Dadi PK, Luo B, Vierra NC, Jacobson DA. TASK-1 potassium channels limit pancreatic α-cell calcium influx and glucagon secretion. Mol Endocrinol 2015;29:777–787
28. Dolatshad H, Biggs D, Diaz R, Hortin N, Preece C, Davies B. A versatile transgenic allele for mouse overexpression studies. Mamm Genome 2015;26:598–608
29. Parker HE, Adriaenssens A, Rogers G, et al. Predominant role of active versus facilitative glucose transport for glucagon-like peptide-1 secretion. Diabetologia 2012;55:2445–2455
30. Schoors S, Bruning U, Missiaen R, et al. Fatty acid carbon is essential for dNTP synthesis in endothelial cells. Nature 2015;520:192–197
31. Carter JD, Dula SB, Corbin KL, Wu R, Nunemaker CS. A practical guide to rodent islet isolation and assessment. Biol Proced Online 2009;11:3–31
32. Pauerstein PT, Park KM, Peiris HS, Wang J, Kim SK. Research resource: genetic labeling of human islet alpha cells. Mol Endocrinol 2016;30:248–253
33. Tantama M, Martínez-François JR, Mongeon R, Yellen G. Imaging energy status in live cells with a fluorescent biosensor of the intracellular ATP-to-ADP ratio. Nat Commun 2013;4:2550
34. Briant LJ, Zhang Q, Vergari E, et al. Functional identification of islet cell types by electrophysiological fingerprinting. J R Soc Interface 2017;14:20160999
35. Smelt MJ, Faas MM, de Haan BJ, de Vos P. Pancreatic beta-cell purification by altering FAD and NAD(P)H metabolism. Exp Diabetes Res 2008;2008:165360
36. Hodek O, Henderson J, Argemi-Muntadas L, Khan A, Moritz T. Structural elucidation of 3-nitrophenylhydrazine derivatives of tricarboxylic acid cycle acids and optimization of their fragmentation to boost sensitivity in liquid chromatography-mass spectrometry. J Chromatogr B Analyt Technol Biomed Life Sci 2023;1222:123719
37. Lindén P, Keech O, Stenlund H, Gardeström P, Moritz T. Reduced mitochondrial malate dehydrogenase activity has a strong effect on photorespiratory metabolism as revealed by ^{13}C labelling. J Exp Bot 2016;67:3123–3135
38. Göpel SO, Kanno T, Barg S, Rorsman P. Patch-clamp characterisation of somatostatin-secreting -cells in intact mouse pancreatic islets. J Physiol 2000;528:497–507
39. Hong J, Abudula R, Chen J, et al. The short-term effect of fatty acids on glucagon secretion is influenced by their chain length, spatial configuration, and degree of unsaturation: studies in vitro. Metabolism 2005;54:1329–1336
40. Olofsson CS, Salehi A, Göpel SO, Holm C, Rorsman P. Palmitate stimulation of glucagon secretion in mouse pancreatic alpha-cells results from activation of L-type calcium channels and elevation of cytoplasmic calcium. Diabetes 2004;53:2836–2843
41. Hoppa MB, Collins S, Ramracheya R, et al. Chronic palmitate exposure inhibits insulin secretion by dissociation of Ca(2+) channels from secretory granules. Cell Metab 2009;10:455–465
42. Wang L, Yuan L, Zeng X, et al. A multisite-binding switchable fluorescent probe for monitoring mitochondrial ATP level fluctuation in live cells. Angew Chem Int Ed Engl 2016;55:1773–1776

43. Ishihara H, Maechler P, Gjinovci A, Herrera PL, Wollheim CB. Islet beta-cell secretion determines glucagon release from neighbouring alpha-cells. Nat Cell Biol 2003;5:330–335
44. McGarry JD, Foster DW. In support of the roles of malonyl-CoA and carnitine acyltransferase I in the regulation of hepatic fatty acid oxidation and ketogenesis. J Biol Chem 1979;254:8163–8168
45. Randle PJ, Garland PB, Hales CN, Newsholme EA. The glucose fatty-acid cycle. Its role in insulin sensitivity and the metabolic disturbances of diabetes mellitus. Lancet 1963;1:785–789
46. Hue L, Taegtmeyer H. The Randle cycle revisited: a new head for an old hat. Am J Physiol Endocrinol Metab 2009;297:E578–E591
47. DiGruccio MR, Mawla AM, Donaldson CJ, et al. Comprehensive alpha, beta and delta cell transcriptomes reveal that ghrelin selectively activates delta cells and promotes somatostatin release from pancreatic islets. Mol Metab 2016;5:449–458
48. Mawla AM, Huising MO. Navigating the depths and avoiding the shallows of pancreatic islet cell transcriptomes. Diabetes 2019;68:1380–1393
49. Pilegaard H, Saltin B, Neufer PD. Effect of short-term fasting and refeeding on transcriptional regulation of metabolic genes in human skeletal muscle. Diabetes 2003;52:657–662
50. Sugden MC, Bulmer K, Augustine D, Holness MJ. Selective modification of pyruvate dehydrogenase kinase isoform expression in rat pancreatic islets elicited by starvation and activation of peroxisome proliferator-activated receptor-α: implications for glucose-stimulated insulin secretion. Diabetes 2001;50:2729–2736
51. Capozzi ME, Svendsen B, Encisco SE, et al. β Cell tone is defined by proglucagon peptides through cAMP signaling. JCI Insight 2019;4: e126742
52. Houten SM, Wanders RJA, Ranea-Robles P. Metabolic interactions between peroxisomes and mitochondria with a special focus on acylcarnitine metabolism. Biochim Biophys Acta Mol Basis Dis 2020;1866:165720
53. Violante S, Achetib N, van Roermund CWT, et al. Peroxisomes can oxidize medium- and long-chain fatty acids through a pathway involving ABCD3 and HSD17B4. FASEB J 2019;33:4355–4364
54. Violante S, Ijlst L, Te Brinke H, et al. Peroxisomes contribute to the acylcarnitine production when the carnitine shuttle is deficient. Biochim Biophys Acta 2013;1831:1467–1474
55. Bokvist K, Olsen HL, Høy M, et al. Characterisation of sulphonylurea and ATP-regulated K+ channels in rat pancreatic A-cells. Pflugers Arch 1999; 438:428–436
56. Schuit F, De Vos A, Farfari S, et al. Metabolic fate of glucose in purified islet cells. Glucose-regulated anaplerosis in beta cells. J Biol Chem 1997;272:18572–18579
57. Östenson C-G. Alloxan reversibly impairs glucagon release and glucose oxidation by pancreatic A2-cells. Biochem J 1980;188:201–206
58. Östenson CG. Regulation of glucagon release: effects of insulin on the pancreatic A2-cell of the guinea pig. Diabetologia 1979;17:325–330
59. Allen DO. Role of albumin in hormone-stimulated lipolysis. Biochem Pharmacol 1979;28:733–736
60. Francis GL. Albumin and mammalian cell culture: implications for biotechnology applications. Cytotechnology 2010;62:1–16
61. Ho RJ, Sutherland EW. Action of feedback regulator on adenylate cyclase. Proc Natl Acad Sci U S A 1975;72:1773–1777
62. Qi C, Sorrentino S, Medalia O, Korkhov VM. The structure of a membrane adenylyl cyclase bound to an activated stimulatory G protein. Science 2019;364:389–394
63. Lubaczeuski C, Bozadjieva-Kramer N, Louzada RA, Gittes GK, Leibowitz G, Bernal-Mizrachi E. Time-dependent effects of endogenous hyperglucagonemia on glucose homeostasis and hepatic glucagon action. JCI Insight 2023;8:e162255
64. Dean ED. A primary role for α-cells as amino acid sensors. Diabetes 2020;69:542–549
65. Prentki M, Corkey BE, Madiraju SRM. Lipid-associated metabolic signalling networks in pancreatic beta cell function. Diabetologia 2020;63:10–20